IEICE TRANSACTIONS

on Communications

DOI:10.23919/transcom.2024EBP3028

This advance publication article will be replaced by the finalized version after proofreading.

A PUBLICATION OF THE COMMUNICATIONS SOCIETY

The Institute of Electronics, Information and Communication Engineers

Kikai-Shinko-Kaikan Bldg., 5-8, Shibakoen 3chome, Minato-ku, TOKYO, 105-0011 JAPAN

PAPER

Analysis of beamforming for OAM communication using loop antenna arrays and paraboloids

Akira SAITOU[†], **Kaito UCHIDA**[†], **Kanki KITAYAMA**[†], **Ryo ISHIKAWA**[†], ***Members***, ***and*** **Kazuhiko HONJO**[†], ***Fellow***

SUMMARY Analytical expression of transmission for the orbital angular momentum (OAM) communication using loop antenna arrays and paraboloids is derived to achieve a communication distance of 100 m. With the field distribution of the single "transformed OAM mode" radiated by a loop antenna, the collimated field by the transmitting paraboloid and its diffracted field are analytically derived. Effects of frequencies, sizes of paraboloids, and shifts of transmitting and receiving arrays from the focal planes are included. With the diffracted field distribution on the focal plane of the receiving paraboloid, transmission between the transmitting and receiving loop antennas is analytically estimated. It is shown that the transmission between the antennas with different OAM modes is null, but the transmission between the antennas with the same mode can be reduced. To clarify the mechanism of the reduction, factors of the reduction are quantitatively defined, and the explicit formulae are derived. Based on the analytical results, numerical estimation for a communication distance of 100 m is demonstrated, where the frequency, the focal length, and the size of the paraboloid are 150 GHz, 50 cm and 100 cm, respectively. Where both arrays are located on each focal plane, the transmission for the signal is more than −7.78 dB for eight kinds of OAM modes. The transmission is the least for the highest-order mode. The transmission loss is shown to be mitigated by optimizing the shifts of transmitting and receiving arrays from their focal planes. The loss is made almost even by exploiting the tradeoff of the improvement for the mode orders. The transmission is improved by 5.98 dB, to be more than −1.80 dB, by optimizing the shifts of the arrays.

key words: *OAM wave, diffraction, eigenmode, paraboloid, numerical calculation*

1. Introduction

A variety of multiplexing methods have been investigated to improve frequency usage efficiency, because frequency bands are precious and finite resources. Whereas the efficiency can be improved within the scope of the Shannon-Hartley theorem, the methods have been exploited only by sacrificing the exponentially increased power. While the MIMO multiplexing communication scheme relaxes the severe demand for the power, it requires complex signal processing to obtain spatially independent channels. On the other hand, the orbital angular momentum (OAM) communication method relaxes the complexity by exploiting the spatial orthogonality of the electromagnetic fields [1]–[7]. An important feature of the OAM eigenmode is its spatial distribution of $\exp(jm\phi)$ in the spherical or cylindrical coordinate system, where m denotes the index that is called the phase mode number or the magnetic quantum number. When different signal sequences are overlaid on n kinds of OAM eigenmodes, n-channel spatial multiplexing becomes possible due to the spatial orthogonality of $\exp(jm\phi)$. Thus, multiplexing in the same frequency band is enabled. In addition, the feature of the eigenmode transmission relaxes the demands for the complexity of signal-processing. As the OAM communication exploits the spatial distribution, the direction of the receiver is strictly specified. Thus, the OAM communication may be anticipated to provide a novel physical dimension of a multiplexing method for the fixed wireless communication.

To obtain pure OAM single-modes, various schemes have been proposed. In the frequency range of light, a spiral phase plate or computer-generated holograms have been used to realize the phase distribution of $\exp(jm\phi)$ [8]–[14], where the plane wave is transformed into the OAM wave.

In the microwave frequency range, a uniform circular array has often been used, where each antenna is stimulated for the phase to be shifted by 2π divided by integers related with the element number of the array [5], [7], [16]–[19]. Whereas the phase distribution of the OAM wave results only at discreet points physically, communication is enabled owing to the sampling theorem. The number of the discreet points can be increased by increasing the number of elements, where feasible modes are also increased. As its element radiation pattern may be arbitrary, flexible configurations of the array can be exploited. Signals are artfully distributed with the Butler Matrix. In addition, dual polarizations can be easily exploited. Thus, the data rate is more than 100 Gbit/s for a communication distance of 100 m, where 15 data streams are exploited at 40 GHz [20].

On the other hand, a continuous field distribution of $\exp(jm\phi)$ has been obtained with a circular travelling antenna in the microwave frequency range, where a cylindrical slot and a stimulation phase-shifted by 90 degrees are exploited [21], [22]. In addition, an OAM communication scheme using loop antennas and paraboloids has been proposed, where the antenna radiates an almost single "transformed OAM mode" directly by controlling the radius of the loop antenna [23], [24]. The transformed mode is a linear combination of $+m^{th}$ and $-m^{th}$ order OAM modes. This mode may be understood as a state in which two kinds of photons, one with an OAM of $m\hbar$ and another with an OAM of $-m\hbar$, are entangled. In addition, its independent mode can be radiated by rotating the port azimuth of the antenna by $\pi/(2m)$, where the radiated field distribution is an independent linear combination of $\pm m^{th}$ order modes [25], [26]. Thus, the number of feasible modes is identical to that for

[†]The authors are with the University of Electro-Communications, Chofu-shi, Tokyo 182-8585, Japan.

Copyright © 200x The Institute of Electronics, Information and Communication Engineers

the other OAM communication schemes. The mode unity is further improved by a reflector plane and port-azimuth control [27], [28]. An array of concentric loop antenna elements radiates plural single-mode waves concurrently, where each wave propagates independently in favor of the spatial orthogonality. For a receiver, the antenna receives only the mode. Thus, an ideal communication is enabled without the troublesome signal-processing, if the diffraction can be neglected for the collimated field.

Whereas the OAM communication has been shown to be effective in the lower frequency bands for short-range communication [23]–[28], higher frequency bands are desirable for long-range communication, such as 100 m in terms of mitigating the diffraction effect. Whereas the diffraction effect has been analyzed also for the uniform circular array scheme [29], [30] to increase the distance, the effect is more complex for the loop antenna scheme, because the received field should be identical to the radiated field distribution for ρ as well as ϕ. This requirement may be said to be a harmful influence of communication without the troublesome signal processing. Thus, to estimate the performance of this scheme, a more-detailed investigation of the diffraction is required. For long-range communication such as 100 m, a large paraboloid and a high frequency would be required, where a prohibitively long time is concerned for simulations.

Thus, the analytical expression of the diffraction of the transformed OAM wave is investigated in this paper. In Section 2, the field distribution is analytically derived for the collimation of the transformed OAM waves with a paraboloid. With the obtained distribution, the diffracted field distribution is analytically derived. In Section 3, the analytical expression of the transmission between the transmitting and receiving loop antennas is obtained. In addition, factors of the transmission loss are investigated to clarify the mechanism. With the obtained analytical expression, the field distributions and transmissions are numerically estimated for a simple case in which the transmitting and receiving arrays are on their focal planes in Section 4. In Section 5, improvement of the transmission is investigated by optimizing the shifts of the arrays away from their focal planes.

2. Collimation and diffraction of transformed OAM wave

The m^{th}-order transformed OAM eigenmode radiated by the loop antenna with the planar reflector is given by (1) and (2), where the circumference of the antenna is adjusted to be the integral multiple of the wavelength [23], [27].

The spherical coordinates are expressed by r', θ' and ϕ', and d denotes the distance between the loop antenna and the planar reflector. The assumed time convention is $\exp(-j\omega t)$. The radiated power is normalized as follows, where η and R denote the wave impedance in free space and the radius of the sphere for the integration, respectively:

$$\mathrm{P_{rad}} = \frac{1}{2\eta}\int_0^{2\pi} d\phi' \int_0^{\frac{\pi}{2}} d\theta' \{R^2 \mathbf{E}_i^{(m)} \cdot \mathbf{E}_i^{(m')^*}\} = \delta_{mm'} \quad (3)$$

Where the center of the loop antenna is shifted by z_{0t} along the Z-axis, the far field $\boldsymbol{E}_1$ is estimated with the Fraunhofer approximation as follows:

$$\mathbf{E}_1 = \exp\{-jkz_{0t}\cos\theta'\}\mathbf{E}_i^{(m)} \quad (4)$$

The far field, shown in (1) and (4), may be interpreted to be radiated from the origin, because it is proportional to $e^{jkr'}/r'$. In this case, the dependence of the magnitude and phase on θ' and ϕ' is given by the equations.

The collimated field of the OAM wave by the paraboloid is analyzed as shown in Fig. 1. The focal point is located at the origin, and the focal length is denoted by f. To collimate all the radiated power, the radius is selected to be $2f$.

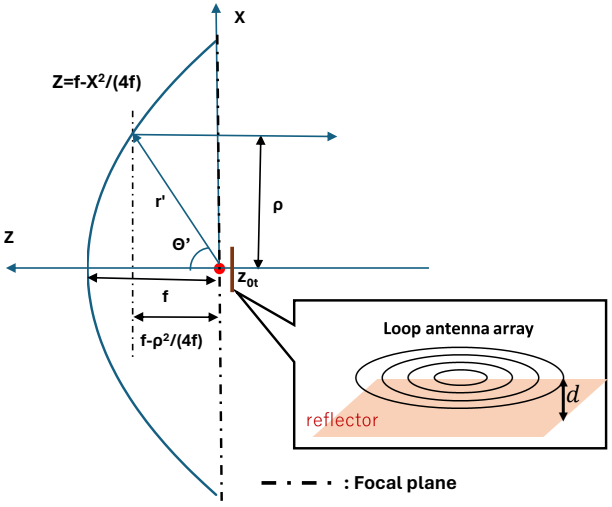

Fig. 1 Configuration of collimation with transmitting paraboloid

Where the collimated field on the focal plane (XY plane) is expressed with a cylindrical coordinate (ρ, ϕ, z), the transformation by the paraboloid is expressed as follows:

$$\mathbf{E}_i^{(m)} = \frac{(-j)^{m-1}\sqrt{\frac{2\eta}{\pi}}\sin(kd\cos\theta')}{A(m)}\frac{e^{jkr'}}{r'}\begin{bmatrix}\approx 0\\ \cot\theta' J_m(m\sin\theta')\sin m\phi' \\ \frac{dJ_m(x)}{dx}|_{x=m\sin\theta'}\cos m\phi'\end{bmatrix} \quad m \geq 0,\ \ 0 \leq \theta' \leq \frac{\pi}{2} \quad (1)$$

$$A(m) \equiv \sqrt{\int_0^{\frac{\pi}{2}}\left[\sin^2(kd\cos\theta')\{\cot^2\theta'(J_m(m\sin\theta'))^2 + (\frac{dJ_m(m\sin\theta')}{dx})^2\}\right]\sin\theta' d\theta'} \quad (2)$$

$$\phi' = \phi \tag{5}$$

$$\sin\theta' = \frac{\rho}{\sqrt{\rho^2 + \left(f - \frac{\rho^2}{4f}\right)^2}} \qquad 0 \le \theta' \le \frac{\pi}{2} \tag{6}$$

The collimated field $\boldsymbol{E}_{\rm ap}$ has been given as follows [31], [32], where the source is at the focal point:

$$\begin{aligned}\mathbf{E}_{\rm ap} &= \begin{bmatrix} [\mathbf{E}_{ap}(\rho,\phi,0)]_\rho \\ [\mathbf{E}_{ap}(\rho,\phi,0)]_\phi \\ [\mathbf{E}_{ap}(\rho,\phi,0)]_z \end{bmatrix} \\ &= -\left(\sqrt{\frac{\varepsilon}{\mu}}\frac{\mathrm{P}_t}{2\pi}\right)^{1/2} \frac{e^{-2jkf}}{\sqrt{\rho^2+f^2}} \begin{bmatrix} \mathrm{G}_\theta(\theta',\phi')^{1/2} \\ \mathrm{G}_\phi(\theta',\phi')^{1/2} \\ 0 \end{bmatrix}\end{aligned} \tag{7}$$

Whereas the loop antenna array is shifted along the Z-axis in the case of (4), the source may be considered to be at the focal point. Thus, the collimated fields $\boldsymbol{E}_{ap}$ of the OAM wave can be estimated with (1), (4) and (7). The gains for the cylindrical coordinate are estimated with (1), (4), (5), and (6). Thus, the collimated field is given by (8).

The collimated field expands by the diffraction, and the diffracted field $\boldsymbol{E}(\rho,\phi,z,m)$ is given by (9) [33], where (ρ,ϕ,z) and (ρ',ϕ',z') denote the coordinates of the observation point and the aperture points on the transmitting focal plane for the cylindrical coordinate system, respectively.

The diffracted field on the receiving focal plane is obtained by substituting (8) for the electric field of (9). In addition, the integration for ϕ' can be analytically obtained, as shown in (10). Thus, the diffracted field is given by the integration only for ρ', as shown in (11).

$$\left.\begin{aligned} &\int_0^{2\pi} \frac{\exp\left(ik\sqrt{\rho^2+\rho'^2-2\rho\rho'\cos(\phi-\phi')+z^2}\right)}{k\sqrt{\rho^2+\rho'^2-2\rho\rho'\cos(\phi-\phi')+z^2}} \sin m\phi' d\phi' \\ &\qquad = g(\rho',\rho,z)\sin m\phi \\ &\int_0^{2\pi} \frac{\exp\left(ik\sqrt{\rho^2+\rho'^2-2\rho\rho'\cos(\phi-\phi')+z^2}\right)}{k\sqrt{\rho^2+\rho'^2-2\rho\rho'\cos(\phi-\phi')+z^2}} \cos m\phi' d\phi' \\ &\qquad = g(\rho',\rho,z)\cos m\phi \\ &g(\rho',\rho,z) \equiv \int_0^{2\pi} \cos m\phi' \\ &\qquad \times \frac{\exp\left(ik\sqrt{\rho^2+\rho'^2-2\rho\rho'\cos(\phi-\phi')+z^2}\right)}{k\sqrt{\rho^2+\rho'^2-2\rho\rho'\cos(\phi-\phi')+z^2}} d\phi' \end{aligned}\right\} \tag{10}$$

$$\begin{aligned}\mathbf{E}(\rho,\phi,z,m) = \frac{2jk^2e^{2jkf}\sqrt{\eta}}{(2\pi)^{3/2}A(m)} \times \\ \begin{bmatrix} \sin m\phi \int_0^{2f} \exp\left[\frac{-jkz_0\left(f-\frac{\rho'^2}{4f}\right)}{\sqrt{\rho'^2+\left(f-\frac{\rho'^2}{4f}\right)^2}}\right] f_1(\rho')g(\rho',\rho,z)d\rho' \\ \cos m\phi \int_0^{2f} \exp\left[\frac{-jkz_0\left(f-\frac{\rho'^2}{4f}\right)}{\sqrt{\rho'^2+\left(f-\frac{\rho'^2}{4f}\right)^2}}\right] f_2(\rho')g(\rho',\rho,z)d\rho' \\ 0 \end{bmatrix}\end{aligned} \tag{11}$$

3. Transmission between loop antennas

The transmission is estimated for a communication distance of z_c, where z_c is defined as the distance between the focal planes of the transmitting and receiving paraboloids. For the receiver, the center of the loop antenna is shifted by z_{0r} along the Z-axis, as shown in Fig. 2. The structures of both the loop antenna array and the paraboloid are identical to those for the transmitter.

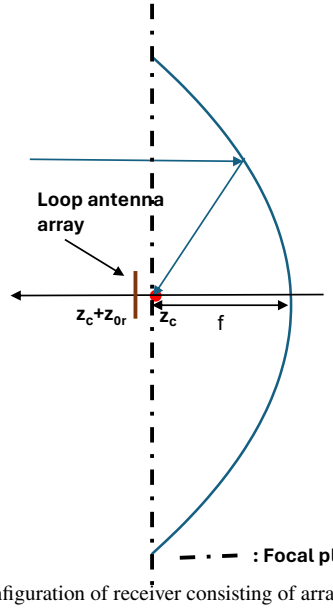

Fig. 2 Configuration of receiver consisting of array and paraboloid

$$\mathbf{E}_{\rm ap}(\rho,\phi,m) = -\frac{\exp\left(2jkf\sqrt{\frac{2\eta}{\pi}}\right)}{A(m)} \exp\left[\frac{jkz_{0r}\left(f-\frac{\rho^2}{4f}\right)}{f+\frac{\rho^2}{4f}}\right] \begin{bmatrix} f_1(\rho)\sin m\phi \\ f_2(\rho)\cos m\phi \\ 0 \end{bmatrix} \qquad 0 \le \rho \le 2f \tag{8}$$

$$f_1(\rho) = \sin\left[\frac{kd\left(f-\frac{\rho^2}{4f}\right)}{f+\frac{\rho^2}{4f}}\right] \frac{f-\frac{\rho^2}{4f}}{\rho\left(f+\frac{\rho^2}{4f}\right)} J_m\left(\frac{m\rho}{f+\frac{\rho^2}{4f}}\right), \quad f_2(\rho) = \sin\left[\frac{kd\left(f-\frac{\rho^2}{4f}\right)}{f+\frac{\rho^2}{4f}}\right] \frac{1}{f+\frac{\rho^2}{4f}} \frac{J_{m-1}\left(\frac{m\rho}{f+\frac{\rho^2}{4f}}\right) - J_{m+1}\left(\frac{m\rho}{f+\frac{\rho^2}{4f}}\right)}{2}$$

$$\mathbf{E}(\rho,\phi,z,m) = \frac{k^2}{j2\pi}\int_0^{2f}\int_0^{2\pi} \begin{bmatrix} (\mathrm{E}_{\rm ap})_{\rho'} \\ (\mathrm{E}_{\rm ap})_{\phi'} \\ 0 \end{bmatrix} \frac{\exp\left[ik\sqrt{\rho^2+\rho'^2-2\rho\rho'\cos(\phi-\phi')+z^2}\right]}{k\sqrt{\rho^2+\rho'^2-2\rho\rho'\cos(\phi-\phi')+z^2}} \rho' d\rho' d\phi' \tag{9}$$

Considering the reciprocal behavior of the field and the current on the antenna, the received field distribution $\boldsymbol{E}_r$ on the receiving focal plane is proportional to (8), except for the phase caused by the shift of the array, as follows:

$$\mathbf{E_r}(\rho,\phi,m) = \sqrt{\frac{2\eta}{\pi}}\frac{1}{A(m)} \times \exp\left[\frac{jkz_{0r}\left(f-\frac{\rho^2}{4f}\right)}{f+\frac{\rho^2}{4f}}\right]\begin{bmatrix} f_1(\rho)\sin m\phi \\ f_2(\rho)\cos m\phi \\ 0 \end{bmatrix} \quad 0 \le \rho \le 2f \tag{12}$$

The constant phase over the focal plane is neglected. In a hypothetical case in which the positions for the transmitting and receiving focal planes are coincident, the magnitude of the transmission would be 0 dB for z_{0r} to be z_{0t}, which implies that the arrays should be shifted toward the same direction along the Z-axis.

As the field distribution on the receiving focal plane is given by (11), the ratio $T^{\text{total}}_{m'm}$ for the transmitted and received power is given by (13), where the OAM mode orders of the transmitting and receiving antennas are m and m', respectively.

The integration terms of the denominator are the total powers identical to the transmitting and receiving focal planes, which are identical to the radiated power shown in (3). Thus, the denominator of (13) is 1.

From (13), the differences of both the magnitude and phase for $\boldsymbol{E}_r$ and $\boldsymbol{E}$ affect the transmission. The numerator of (14) is proportional to the received power. Where the phase distributions of $\boldsymbol{E}$ and $\boldsymbol{E}_r$ are identical, it becomes the denominator. It should be noted that constant phase difference does not affect the value of (14). Thus, the effect of the phase distribution difference, T^{phase}, can be estimated as follows:

$$T^{\text{phase}} = \left|\frac{\int_0^{2\pi}\left[\int_0^{2f}(\mathbf{E}_r(\rho,\phi,m)^*\cdot\mathbf{E}(\rho,\phi,z_c,m))\rho d\rho\right]d\phi}{\int_0^{2\pi}\left[\int_0^{2f}|\mathbf{E}_r(\rho,\phi,m)^*\cdot\mathbf{E}(\rho,\phi,z_c,m)|\rho d\rho\right]d\phi}\right|^2 \tag{14}$$

The collection ratio by the receiving paraboloid, T^c, is given by the power portion inside the radius of the paraboloid ($2f$) for the diffracted field as follows:

$$T^c = \frac{\int_0^{2\pi}[\int_0^{2f}|\mathbf{E}(\rho,\phi,z_c)|^2\rho d\rho]d\phi}{\int_0^{2\pi}[\int_0^{\infty}|\mathbf{E}(\rho,\phi,z_c)|^2\rho d\rho]d\phi} \tag{15}$$

The residual loss of transmission, T^{mag}, is assumed to be the effect of the magnitude difference, as follows:

$$T^{\text{mag}} = T^{\text{phase}}\cdot T^c / T^{\text{total}} \tag{16}$$

By substituting (11) and (12) in (13)–(15), definite equations are obtained, as shown in (17)–(19).

$$T^{\text{total}}_{mm'} = \frac{k^4\pi^2}{8\eta}\delta_{mm'} \times \left|\int_0^{2f}\exp\left[\frac{-jkz_{0r}(f-\frac{\rho^2}{4f})}{f+\frac{\rho^2}{4f}}\right]\{f_1(\rho)f_3(\rho)+f_2(\rho)f_4(\rho)\}\rho d\rho\right|^2 \tag{17}$$

$$T^{\text{phase}} = \left|\frac{\int_0^{2f}\exp\left[\frac{-jkz_{0r}(f-\frac{\rho^2}{4f})}{f+\frac{\rho^2}{4f}}\right]\{f_1(\rho)f_3(\rho)+f_2(\rho)f_4(\rho)\}\rho d\rho}{\{\int_0^{2f}|f_1(\rho)f_3(\rho)+f_2(\rho)f_4(\rho)|\rho d\rho\}^2}\right|^2 \tag{18}$$

$$T^c = \frac{k^4}{8\pi\eta}\int_0^{2f}\left\{|f_3(\rho)|^2+|f_4(\rho)|^2\right\}\rho d\rho \tag{19}$$

$$\left.\begin{aligned} f_3(\rho) &= \int_0^{2f}\exp\left[\frac{-jkz_{0t}\left(f-\frac{\rho'^2}{4f}\right)}{f+\frac{\rho'^2}{4f}}\right]f_1(\rho')g(\rho',\rho,z_c)\rho' d\rho' \\ f_4(\rho) &= \int_0^{2f}\exp\left[\frac{-jkz_{0t}\left(f-\frac{\rho'^2}{4f}\right)}{f+\frac{\rho'^2}{4f}}\right]f_2(\rho')g(\rho',\rho,z_c)\rho' d\rho' \end{aligned}\right\} \tag{20}$$

Kronecker delta is denoted by $\delta_{mm'}$. From (17), the loop antennas of the other OAM modes receive no power, because the field distribution along ϕ of each OAM mode is maintained after the diffraction. The transmission loss is caused by the different field distribution along ρ. Thus, whereas interference waves are not generated, the signal wave can be attenuated for an OAM communication scheme using loop antennas. From (18), the effect of the phase

$$\begin{aligned} T^{\text{total}}_{m'm} &= \left|\frac{\frac{1}{2\eta}\int_0^{2\pi}\left[\int_0^{2f}(\mathbf{E}_r(\rho,\phi,m')^*\cdot\mathbf{E}(\rho,\phi,z_c,m))\rho d\rho\right]d\phi}{\frac{1}{2\eta}\sqrt{\int_0^{2\pi}\left[\int_0^{2f}|\mathbf{E}_r(\rho,\phi,m')|^2\rho d\rho\right]d\phi\cdot\int_0^{2\pi}\left[\int_0^{\infty}|\mathbf{E}(\rho,\phi,z_c,m)|^2\rho d\rho\right]d\phi}}\right|^2 \\ &= \left|\frac{\int_0^{2\pi}\left[\int_0^{2f}(\mathbf{E}_r(\rho,\phi,m)^*\cdot\mathbf{E}(\rho,\phi,z_c,m))\rho d\rho\right]d\phi}{2\eta}\right|^2 \end{aligned} \tag{13}$$

difference can be partly mitigated by controlling the value of z_{0r}.

4. Numerical calculation for transmitting and receiving arrays located on each focal plane

To estimate the proper values for the frequency and the focal length, simple configurations are numerically calculated with Mathematica™, where the transmitting and receiving arrays are located on each focal plane. To achieve a communication distance of 100 m for OAM modes up to the 8^{th} order, the values were selected to be 150 GHz and 50 cm, respectively, after preliminary calculations. The radius of the paraboloid is $2f$, as explained in Section 2.

As the diffraction effect is larger for higher-order modes, the calculated field distributions for the 8^{th}-order OAM mode are shown in Fig. 3 for a communication distance, z_c, of 100 m. Fig. 3 (a) shows the magnitudes of θ'- and ϕ'-polarized radiated fields and their accumulated power. Fig. 3 (b) shows the magnitudes of collimated ρ- and ϕ-polarized fields and their accumulated power up to ρ. Whereas the fields are dependent on $\sin m\phi$ or $\cos m\phi$, as shown in (8), the dependence is removed. Thus, they correspond to the magnitudes where $\sin m\phi$ or $\cos m\phi$ is ± 1. For arbitrary ϕ, the magnitudes are obtained by multiplying $|\sin m\phi|$or $|\cos m\phi|$. As the radius of the paraboloid is 100 cm ($2f$), the accumulated power becomes identical to the radiated power at a ρ of 100 cm. The phase distribution is not shown, because it is constant over ρ, as shown in (8). Fig. 3(c) and (d) show the magnitudes and phases of the diffracted fields on the receiving focal plane, respectively. The positions of the maximum magnitudes move about 20 cm outward by the diffraction, and the accumulated power up to the radius of the receiving paraboloid becomes slightly less than 1 W. Whereas the phase is constant at the transmitting focal plane, the phases increase with ρ by the diffraction. From (8) and (12), the magnitude of the received field distribution is identical to the collimated field shown in Fig. 3 (b). In addition, as the receiving array is on its focal plane, the phase distribution of the received field is constant. Thus, the differences of the phase distributions for T^{phase} are identical to those shown in Fig. 3 (d).

Table 1 and Figure 4 show the transmission characteristics explained in (13)–(16). To clarify the effect of the

Table 1 Transmission characteristics for m

m	T^c (dB)	T^{phase} (dB)	T^{mag} (dB)	T_{mm}^{total} (dB)
1	−0.05	−0.89	−0.73	−1.66
2	−0.01	−1.05	−0.47	−1.54
3	−0.01	−1.44	−0.56	−2.01
4	−0.02	−1.96	−0.79	−2.76
5	−0.02	−2.57	−1.14	−3.74
6	−0.03	−3.24	−1.64	−4.91
7	−0.04	−3.94	−2.28	−6.26
8	−0.06	−4.62	−3.10	−7.78

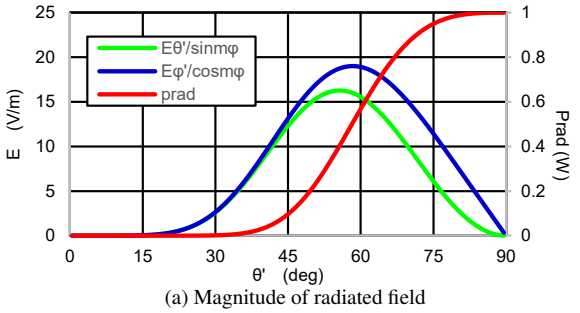

(a) Magnitude of radiated field

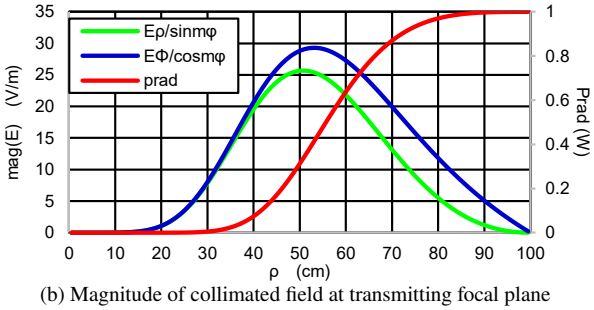

(b) Magnitude of collimated field at transmitting focal plane

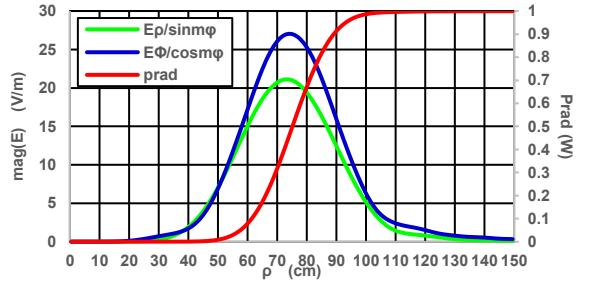

(c) Magnitude of diffracted field at receiving focal plane

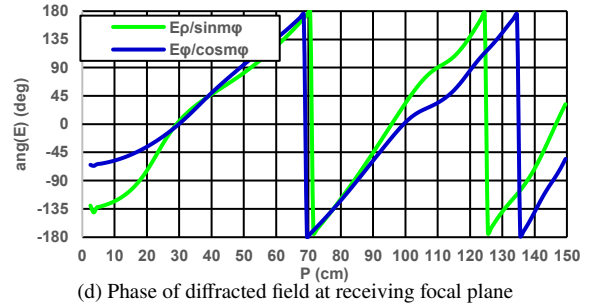

(d) Phase of diffracted field at receiving focal plane

Fig. 3 Calculated field distributions.
freq. = 150 GHz, f = 50 cm, z_c = 100 m, m = 8

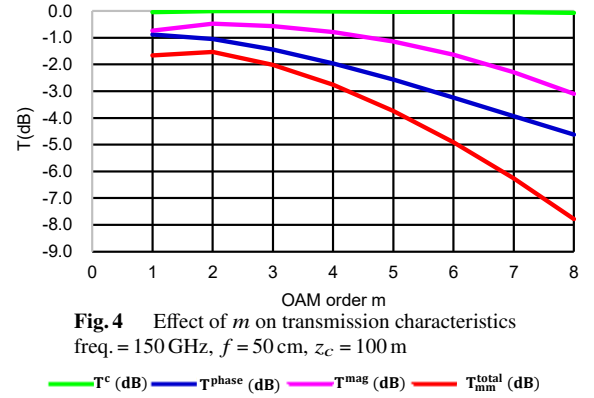

Fig. 4 Effect of m on transmission characteristics
freq. = 150 GHz, f = 50 cm, z_c = 100 m

mode order, the characteristics for the 1^{st} to 8^{th} orders are compared. The loss for T^c is less than 0.1 dB, because the radius of the receiving paraboloid is as large as 100 cm and the frequency is as high as 150 GHz. T^{phase} is the largest factor to decrease the transmission. It is −4.62 dB for the 8^{th} order, which is explained by the phase difference shown in Fig. 3 (d). T^{mag} is −3.10 dB, which is explained by the magnitude difference shown in Figs. 3 (b) and (c). The total transmission, $T^{\text{total}}_{8,8}$, is −7.78 dB. The overall tendency for the modes is that both the total transmission and the factors decrease with the orders. However, only the transmissions for the 1^{st} order are slightly reduced, especially for T^{mag}, because the magnitudes of the fields change drastically during the propagation. Indeed, whereas the magnitude of the field is the maximum at ρ of 0 on the transmitting focal plane, it is null on the receiving focal plane, as shown in Fig. 5. Nevertheless, the OAM mode is maintained, because the difference is related to the distribution along ρ. The OAM mode is totally determined by the distribution along ϕ. Thus, even where the signal is attenuated, the interference does not appear, as already shown in (17).

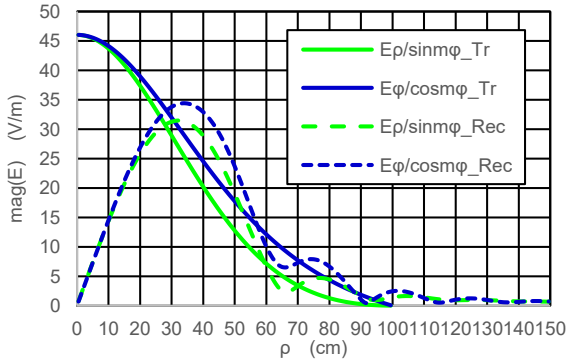

Fig. 5 Magnitudes of fields on transmitting and receiving focal planes $m = 1$, freq. = 150 GHz, $f = 50$ cm, $z_c = 100$ m

5. Improvement of transmission by optimizing shifts

For the simple configuration shown in Section 4, whereas the power is almost wholly collected by the receiving paraboloid, the received power ratio was only −7.8 dB for the 8^{th} order. To improve transmission, we tried to reduce the largest factor of the phase distribution difference. It can be reduced by controlling the shift of the receiving array, as explained in Section 3. In this case, whereas the phase of the received field, $\boldsymbol{E}_r(\rho, \phi, m)$, changes, the magnitude remains identical, as shown in (12). In addition, the field distribution on the receiving focal plane, $\boldsymbol{E}(\rho, \phi, z, m)$, is identical. Thus, both T^c and T^{mag} remain identical, and only T^{phase} changes. Fig. 6 shows the differences in the phases for $\boldsymbol{E}_r(\rho, \phi, m)$ and $\boldsymbol{E}(\rho, \phi, z_c, m)$, where z_{0r} is $0.005f$. The phase differences are almost constant when compared with those shown in Fig. 3 (d). As a result, the calculated T^{phase} is reduced to −0.13 dB, where it is improved by 4.49 dB. $T^{\text{total}}_{8,8}$ becomes

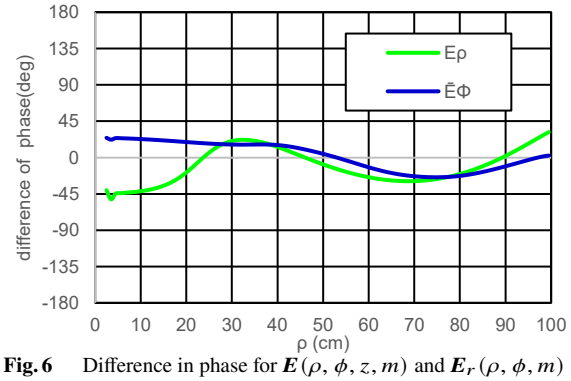

Fig. 6 Difference in phase for $\boldsymbol{E}(\rho, \phi, z, m)$ and $\boldsymbol{E}_r(\rho, \phi, m)$ $m = 8$, freq. =150 GHz, f =50 cm, $z_c = 100$ m, $z_{0r} = 0.005f$

Table 2 Transmission characteristics for m
freq. = 150 GHz, $f = 50$ cm, $z_c = 100$ m, $z_{0r} = 0.005f$

m	T^c (dB)	T^{phase} (dB)	T^{mag} (dB)	T^{total}_{mm} (dB)
1	−0.05	−2.31	−0.73	−3.09
2	−0.01	−2.63	−0.47	−3.12
3	−0.01	−2.13	−0.56	−2.70
4	−0.02	−1.46	−0.79	−2.27
5	−0.02	−0.90	−1.14	−2.06
6	−0.03	−0.49	−1.64	−2.16
7	−0.04	−0.24	−2.28	−2.57
8	−0.06	−0.13	−3.10	−3.29

−3.29 dB, as shown in Table 2. This implies that phase distribution caused by the diffraction is almost compensated for by the receiving array shift of z_{0r}.

However, the phase distribution caused by the diffraction depends on the mode order, and the same phase compensation by z_{0r} overcancels the phase for the lower-order modes. Table 2 also shows the T^{phase} for the other orders.

Whereas T^{phase} is improved remarkably for the 8 th-order mode compared with that in Table 1, it becomes worse for the 1^{st}-, 2^{nd}-, and 3^{rd}-order modes. The obtained total transmissions are more even, and may be more convenient for communication. However, where the transmissions for the lower-order modes are more important, the value of z_{0r} should be decreased.

Next, the improvement of T^{mag} is examined. As the difference in the magnitude distributions is mainly caused by the outward shift of the maximum field position, a slight focusing of the radiated field with the transmitting paraboloid was examined. In this case, the focused beam expands less by the diffraction, and the maximum field position on the receiving focal plane, can be expected to be reduced. To compare the obtained values of T^{mag} with those in Table 1, the receiving array is kept on the focal plane.

Fig. 7 shows the magnitudes of the diffracted fields on the receiving focal plane for varied z_{0t}. To compare the distribution, the received field is also shown. Where the magnitude of the diffracted field is identical to that of the received field, T^{mag} becomes 0 dB. The position of the peak

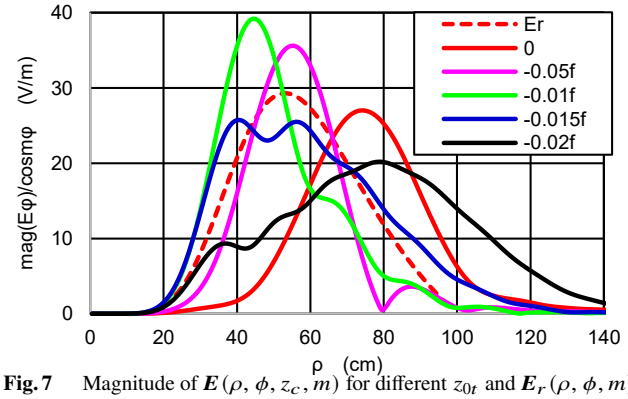

Fig. 7 Magnitude of $\boldsymbol{E}(\rho, \phi, z_c, m)$ for different z_{0t} and $\boldsymbol{E}_r(\rho, \phi, m)$
$m = 8$, freq. = 150 GHz, $f = 50$ cm, $z_c = 100$ m, $z_{0r} = 0$ cm
Numerical values in the legend show the values of z_{0t}.

is reduced when z_{0r} changes from 0 to $-0.01f$; however, it increases thereafter, and the distribution tends to broaden remarkably. As a result, the tail of the distribution exceeds the end of the receiving paraboloid, and the collection ratio of T^c increases, as shown in Table 3 and Fig. 8. In the cases of $-0.005f$ and $-0.015f$ for z_{0t}, the distribution is similar to that of $\boldsymbol{E}_r$, and each T^{mag} is reduced. Thus, T^{mag} can be reduced by reducing the difference of the magnitude distribution. However, in the case of $-0.015f$, the T^{phase} is much larger. Thus, the shift of $-0.005f$ is concluded to be optimal for the 8^{th}-order mode. In this case, T^{mag} is improved by 2.75 dB, and T^{phase} is additionally improved by 1.68 dB, which results in a 4.49 dB improvement to T_{88}^{total}.

Table 3 Effect of z_{0t} on transmission characteristics
freq. = 150 GHz, $f = 50$ cm, $z_c = 100$ m, $z_{0r} = 0.005f$

z_{0t}/f	T^c (dB)	T^{phase} (dB)	T^{mag} (dB)	T_{88}^{total} (dB)
0	−0.06	−4.62	−3.10	−7.78
−0.005	0.00	−2.94	−0.35	−3.29
−0.01	0.00	−9.02	−0.51	−9.53
−0.015	−0.06	−26.56	−0.41	−27.02
−0.02	−0.92	−40.13	−3.08	−44.13

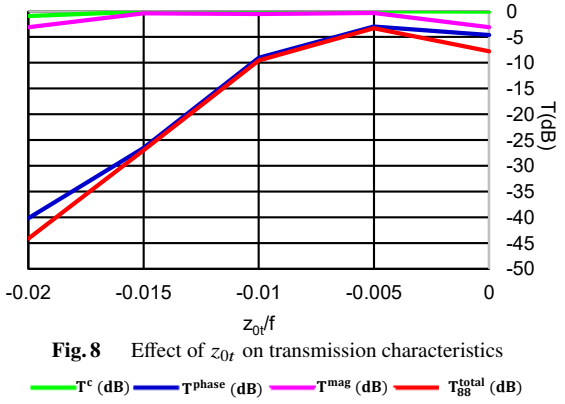

Fig. 8 Effect of z_{0t} on transmission characteristics

The contribution of T^{phase} has been shown to be improved by controlling z_{0r}, where z_{0t} is null. However, the improvement is complicated in the case of nonzero z_{0t}, because the phase difference depends both on z_{0t} and z_{0r} as well as the mode order. By iterating calculations, one of the best characteristics was obtained for the eight kinds of orders, as shown in Table 4. The values of z_{0t} and z_{0r} are $-0.0025f$ and $0.0025f$, respectively. The value of z_{0t} is considerably smaller than the optimum value for the 8^{th}-order mode to improve the transmissions for the lower-order modes. The worst transmission for the eight kinds of modes is −1.8 dB, which is better by 5.98 dB than that shown in Table 1.

Table 4 Transmission characteristics for appropriate z_{0t} and z_{0r}
freq. = 150 GHz, $f = 50$ cm, $z_c = 100$ m, $m_t = 8$, $z_{0t} = 0.0025f$,
$z_{0r} = 0.0025f$

m	T^c (dB)	T^{phase} (dB)	T^{mag} (dB)	T_{mm}^{total} (dB)
1	−0.04	−1.22	−0.53	−1.80
2	−0.00	−1.11	−0.38	−1.50
3	−0.00	−0.70	−0.30	−1.01
4	−0.00	−0.32	−0.24	−0.56
5	−0.00	−0.11	−0.22	−0.34
6	−0.01	−0.10	−0.30	−0.41
7	−0.01	−0.26	−0.50	−0.77
8	−0.01	−0.57	−0.85	−1.44

6. Conclusion

An analytical expression of transmission for OAM communication using loop antenna arrays and paraboloids was derived to achieve a communication distance of 100 m. With the field distribution of the single "transformed OAM mode" radiated by a loop antenna, the collimated field by the transmitting paraboloid and its diffracted field were analytically derived. The effects of frequencies, sizes of paraboloids, and the shifts in transmitting and receiving arrays away from their focal planes were included. With the diffracted field distribution on the focal plane of the receiving paraboloid, the transmission between the transmitting and receiving loop antennas was analytically estimated. It was shown that the transmission between antennas with different OAM modes was null, but the transmission between antennas with the same mode could be reduced. To clarify the mechanism of the reduced transmission, the factors of the reduction were quantitatively defined, and the explicit formulae were derived. Based on the analytical results, numerical estimation for a communication distance of 100 m was demonstrated, where the frequency, the focal length, and the size of the paraboloid were 150 GHz, 50 cm and 100 cm, respectively. Where both arrays were located on each focal plane, the transmission for the signal was more than −7.78 dB for eight kinds of OAM modes, where the transmission was the least for the highest order mode. The transmission loss was shown to be reduced by optimizing the shifts of the transmitting and

receiving arrays away from their focal planes. The loss was made almost even by exploiting the tradeoff of the improvement for the mode orders. The transmission was improved by 5.98 dB, to more than −1.80 dB, by optimizing the shifts of the arrays.

Acknowledgments

This work is partly funded by Ministry of Internal Affairs and Communications, Japan, for SCOPE Programme (#JP225003001).

References

[1] L. Allen, M. W. Beijersbergen, R. J. C. Spreeuw, J. P. Woerdman, "Orbital angular momentum of light and the transformation of Laguerre Gaussian laser modes," Phys. Rev. A., Vol. 45, No. 11, pp. 8185-8189, June 1992

[2] H. He, M. E. J. Friese, N. R. Heckenberg, H. Rubinsztein-Dunlop, "Direct observation of transfer of angular momentum to absorptive particles from a laser beam with a phase singularity," Phys. Rev. Lett., Vol. 75, No. 5, pp. 826 – 829, July 1995

[3] S. Franke-Arnold, L. Allen, M. Padgett, "Advances in optical angular momentum," Laser Photon. Rev., Vol. 2, No. 4, pp. 299-313, July 2008

[4] J. Wang, Jeng-Yuan Yang, I. M. Fazal, N. Ahmed, Y. Yan, H. Huang, Y. Ren, Y. Yue, S. Dolinar, M. Tur, A. E. Willner, "Terabit free-space data transmission employing orbital angular momentum multiplexing," Nature photonics, Vol. 6, pp. 488-496, July 2012

[5] S. M. Mohammadi, L. K. S. Daldorff, J. E. S. Bergman, R. L. Karlsson, B. Thidé, K. Forozesh, T. D. Carozzi, B. Isham," Orbital Angular momentum in Radio- A system study," IEEE Trans. ant. & propaga., Vol. 58, No. 2, pp. 565-572, Feb. 2010

[6] F. Tamburini, E. Mari, A. Sponselli, B. Thidé, A. Bianchini, F. Romanato, "Encoding many channels on the same frequency through radio vorticity: first experimental test," New J. Physics 14, pp. 1-17, March 2012

[7] D. Lee, H. Sasaki, H. Fukumoto, K. Hiraga, T. Nakagawa, "Orbital Angular Momentum (OAM) Multiplexing: An Enabler of a New Era of Wireless Communications," IEICE Trans. Commun., Vol. E100-B, No. 7, pp. 1044-1063, July 2017.

[8] M. W. Beijersbergen, R. P. C. Coerwinkel, M, Kristensen, J. P. Woerdman, "Helical-wavefront laser beams produced with a spiral phaseplate" Opt. commun. Vol. 112, pp. 321-327, 1994.

[9] G. A. Turnbull, D. A. Robertson, G. M. Smith, L. Allen, M. J. Padgett, "The generation of free-space Laguerre-Gaussian modes at millmetre-wave frequencies by use of a spiral phaseplate," Opt. commun. Vol. 127, pp. 183-188, 1996.

[10] S. Tao, X. Yuan, and J. Lin, "Sequence of focused optical vortices generated by a spiral fractal zone plate," Appl. Phys. Lett., vol. 89, no. 3, pp. 1758–1767, 2006.

[11] A. Ostrovsky, C. Rickenstorff, and V. Arrizon, "Generation of the perfect optical vortex using a liquid crystal spatial light modulator," Opt. Lett., vol. 38, no. 4, pp. 534–536, 2013.

[12] X. Su, H. Zhou, K. Zou, A. Minoofar, H. Song, R. Zhang, K. Pang, H. Song, N. Hu, Z. Zhao, A. Almaiman, S. Zach, M. Tur, A. F. Molisch, H. Sasaki, D. Lee, A. E. Willner," Demonstration of 8-Channel 32-Gbit/s QPSK Wireless Communications at 0.28-0.33 THz Using 2 Frequency, 2 Polarization, and 2 Mode Multiplexing," Opt. Fiber Commu. Conf. 2021.

[13] N. R. Heckenberg, R. McDuff, C. P. Smith, H. Rubinsztein-Dunlop & M. J. Wegener, "Laser beams with phase singularities," Opt. Quantum Electronics Vol. 24, pp. 951-962, 1992.

[14] Z. Guo, S. Qu, and S. Liu, "Generating optical vortex with computer-generated hologram fabricated inside glass by femtosecond laser pulses," Opt. Commun., vol. 273, no. 1, pp. 286–289, May 2007.

[15] A. Carpentier, H. Michinel, and J. Salgueiro, "Makling optical vortices with computer-generated holograms," Amer. J. Physics, vol. 76, no. 10, pp. 916–921, 2008.

[16] B. Thidé, H. Then, J. Sjoholm, K. Palmer, J, Bergman, T. D. Carozzi, Ya. N. Istomin, "Utilization of Photon Orbital Angular Momentum in the low-frequency radio domain," Phys. Rev. Lett, 99, 087701, 2007.

[17] Q. Bai, A. Tennant and B. Allen, "Experimental circular phased array for generating OAM radio beams," elec. et, Vol. 50, No. 20, pp. 1414–1415, 2014.

[18] D. Lee H. Sasaki, H Fukumoto, Y. Yagi, T Kaho, H. Shiba, T. Shimizu, "An experimental demonstration of 28 GHz band wireless OAM-MIMO (Orbital Angular Momentum Multi-Input and Multi-Output) multiplexing," Proc. IEEE 87th Veh. Technol. Conf., pp. 1–5, 2018.

[19] Y. Yagi, H. Sasaki, T. Yamada, and D. Lee, "200 Gbit/s wireless transmission using dual-polarized OAM-MIMO multiplexing on 28 GHz band," Proc. IEEE GLOBECOM Workshop, pp. 1–4, 2019.

[20] D. Lee, H. Sasaki, Y. Yagi, H. Shiba, "Orbital Angular Momentum Multiplexing Using Radio Wave and its Extension to Multishape Radio," J. Lightwave Tech. VOL. 41, NO. 7, 2023.

[21] S. Zheng, X. Hui, X. Jin, H. Chi, and X. Zhang, "Transmission characteristics of a twisted radio wave based on circular traveling-wave antenna," IEEE Trans. Antenna Propag., vol. 63, no. 4, pp. 1530-1536, 2015.

[22] W. Zhang, S. Zheng, X. Hui, Y. Chen, X. Jin, H. Chi, X. Zhang, "Four-OAM-mode antenna with traveling-wave ring-slot structure," IEEE Ant. & Wireless Propag. Lett., Vol. 16, pp. 194-197, 2017

[23] A. Saitou, R. Ishikawa, K. Honjo, "4-value multiplexing orbital-angular-momentum communication scheme using loop-antenna arrays," APMC, Dec. 2016.

[24] H. Otsuka, R. Yamagishi, A. Saitou, R. Ishikawa, K. Honjo, "Analytical and Measured Estimation for 4-value Multiplexing OAM Communication Using Loop Array Antennas," European Microw. Conf., Oct. 2017

[25] A. Saitou, H. Otsuka, Y. Yamagishi, R. Ishikawa, H. Suzuki, K. Honjo, "Double Multiplicity Exploiting Orthogonal Polarizations of OAM-Wave for OAM Communication with Loop Arrays," Proc. APMC, pp. 494-496, Nov. 2018

[26] H. Miyake, A. Saitou, H. Suzuki, R. Ishikawa, K. Honjo," Improved Performance for 8-Channel Multiplexing OAM Communication by Suppressing Interference," Proc. 2020 Asia Pacific Mic. Conf., pp.161-163, Dec.9, 2020.

[27] Y. Yamagishi, H. Otsuka, A. Saitou, R. Ishikawa, K. Honjo, " Improvement of mode uniqueness for OAM communication using loop array with reflector plane," Proc. APMC, 2017.

[28] H. Otsuka, Y. Yamagishi, A. Saitou, H. Suzuki, R. Ishikawa, K. Honjo," High performance OAM communication exploiting port-azimuth effect of loop antennas," IEICE Trans. Commun. Vol. E102-B, No12, pp. 2267-2275, Dec. 2019.

[29] T. Nguyen, R. Zenkyu, M. Hirabe, T. Maru, E. Sasaki, "A study of Orbital angular momentum generated by parabolic reflector with circular array feed," Proc. ISAP, pp. 708-709, 2016

[30] S. Saito, Y. Yagi, D. Lee, F, Maehara, "Link distance and carrier frequency dependence of propagation attenuation in OAM multiplexing using parabolic antenna," IEEE, PIMRC, Oct. 2023.

[31] C. A. Balanis, Antenna Theory 3rd ed., pp. 883–937, U. S., J. Wiley & Sons, 1999.

[32] S. Silver, Microwae antenna theory and design, pp. 413-464, McGraw-Hill, 2008.

[33] M. Born, E. Wolf, Principles of optics, 7th Expanded Ed., pp. 436-443, Cambridge University Press, U. K., 2002.

Akira Saitou received his B.E. and M.E. degrees in applied physics from the University of Tokyo in 1975 and 1977, respectively, and his D.E. degree from the University of Electro-Communications in 2008. From 1977 to 2002, he was employed at NEC Corporation to develop GaAs FETs and MMICs for microwave and millimeter-wavecommunication. From 2002-2009, he worked for YKC Corporation to develop microwave circuits and antennas. In 2009, he joined the University of Electro-Communications as a guest professor to develop wideband, dual-band, and OAM antennas.

Kaito Uchida received the B.E. degree in chemical engineering from the Gunma University, Kiryu, Japan in 2022 and is currently working toward the M.E. degree at the University of Electro-communications, Tokyo, Japan.

Kanki Kitayama received the B.E. degree in infomation and commuication engineering from the University of Electro-commuications, Tokyo, Japan in 2023 and is currently working toward the M.E. degree at the University of Electro-communications.

Ryo Ishikawa received the B.E., M.E., and D.E. degrees in electronic engineering from Tohoku University, Sendai, Japan, in 1996, 1998, and 2001, respectively. In 2001, he joined the Research Institute of Electrical Communication, Tohoku University, Sendai, Japan. In 2003, he joined the University of Electro-Communications, Tokyo, Japan. His research interest is the development of microwave compound semiconductor devices and related techniques. Dr. Ishikawa is a member of the Japan Society of Applied Physics. He was the recipient of the 1999 Young Scientist Award for the Presentation of an Excellent Paper of the Tohoku Chapter, Japan Society of Applied Physics.

Kazuhiko Honjo received the B.E. degree from the University of Electro-Communications, Tokyo, in 1974, and the M.E. and D.E. degrees in electronic engineering from the Tokyo Institute of Technology, Tokyo, in 1976 and 1983, respectively. From 1976 to 2001, he worked for NEC Corporation, Kawasaki, Japan. In 2001, he joined the University of Electro-Communications as a professor in the Information and Communication Engineering Department. He has been involved in research and development of high-power/broadband/low-distortion microwave amplifiers, MMICs, HBT device and processing technology, miniature broadband microwave antennas and FDTD electro-magnetic wave and device co-analysis. Prof. Honjo received both the 1983 Microwave Prize and the 1988 Microwave Prize granted by the IEEE Microwave Theory and Techniques Society. He also received the 1980 Young Engineer Award, and the 1999 Electronics Award both presented by the Institute of Electrical, Information and Communication Engineers (IEICE), Japan. He is Life Fellow of IEEE.